Published in final edited form as:
Biochim Biophys Acta. 2015 February ; 1853(2): 396–408. doi:10.1016/j.bbamcr.2014.11.012.

Endothelial Nlrp3 Inflammasome Activation Associated with Lysosomal Destabilization during Coronary Arteritis

Yang Chen[1], **Xiang Li**[1], **Krishna M. Boini**[1], **Ashley L. Pitzer**[1], **Erich Gulbins**[2], **Yang Zhang**[1], and **Pin-Lan Li**[1]

[1]Department of Pharmacology & Toxicology, School of Medicine, Virginia Commonwealth University, Richmond, VA 23298

[2]Department of Molecular Biology, University of Duisburg-Essen, Essen, Germany

Abstract

Inflammasomes play a critical role in the development of vascular diseases. However, the molecular mechanisms activating the inflammasome in endothelial cells and the relevance of this inflammasome activation is far from clear. Here, we investigated the mechanisms by which Nlrp3 inflammasome is activated to result in endothelial dysfunction during coronary arteritis by *Lactobacillus casei* (*L. casei)* cell wall fragments (LCWE) in a mouse model for Kawasaki disease. Endothelial dysfunction associated with increased vascular cell adhesion protein 1 (VCAM-1) expression and endothelial-leukocyte adhesion was observed during coronary arteritis in mice treated with LCWE. Accompanied with these changes, the inflammasome activation was also shown in coronary arterial endothelium, which was characterized by a marked increase in caspase-1 activity and IL-1β production. In cultured endothelial cells, LCWE induced Nlrp3 inflammasome formation, caspase-1 activation and IL-1β production, which were blocked by *Nlrp3* gene silencing or lysosome membrane stabilizing agents such as colchicine, dexamethasome, and ceramide. However, a potassium channel blocker glibenclamide or an oxygen free radical scavenger N-Acetyl-L-cysteine had no effects on LCWE-induced inflammasome activation. LCWE also increased endothelial cell lysosomal membrane permeability and triggered lysosomal cathepsin B release into cytosol. Silencing cathepsin B blocked LCWE-induced Nlrp3 inflammasome formation and activation in endothelial cells. *In vivo*, treatment of mice with cathepsin B inhibitor also abolished LCWE-induced inflammasome activation in coronary arterial endothelium. It is concluded that LCWE enhanced lysosomal membrane permeabilization and consequent release of lysosomal cathepsin B, resulting in

Correspondence should be addressed to: Yang Zhang, Ph.D, Department of Pharmacology & Toxicology, School of Medicine, Virginia Commonwealth University, Richmond, VA 23298; Tel: (804) 828-0738; Fax: (804) 828-4794; yzhang3@vcu.edu Or Pin-Lan Li, M.D, Ph.D, Department of Pharmacology & Toxicology, School of Medicine, Virginia Commonwealth University, Richmond, VA 23298; Tel: (804) 828-4793; Fax: (804) 828-4794; pli@vcu.edu.

Disclosures
None.

activation of endothelial Nlrp3 inflammasome, which may contribute to the development of coronary arteritis.

Keywords

Nlrp3 Inflammasome; LCWE; Endothelium; Lysosomal membrane permeabilization; Cathepsin B

INTRODUCTION

Recently, a new concept is emerging that activation of the inflammasomes, in particular, the Nlrp3 (nucleotide-binding domain and leucine-rich repeat pyrin domain containing 3) inflammasome, plays a critical role in the development of vascular diseases [1–3]. It has been known that the Nlrp3 inflammasome usually consists of three main components including Nlrp3 that functions as pattern recognition receptor, the adaptor protein, ASC (apoptotic speck-containing protein with a CARD) and inactive pro-caspase-1 protein [4]. This inflammasome serves as intracellular machinery responsible for the production of important pro-inflammatory cytokines such as interleukin-1β (IL-1β) and interleukin-18 (IL-18) [5, 6], thereby producing inflammatory response. Recently, Nlrp3 inflammasome activation has also been reported to produce the regulatory or pathogenic actions in cells or tissues beyond the classical inflammatory response. These actions beyond inflammation include pyroptosis, a specific form of cell death that combines characteristics of apoptotic and necrotic death pathways [7–9], changes in cell membrane permeability by enzymatic reaction [10], interference with cytoskeleton arrangement [11], and direct inhibition of functional protein synthesis and metabolism in cells with activated inflammasomes. There is increasing evidence that these non-inflammatory actions of inflammasome activation may also be important in the regulation of cell function and in the mediation of different diseases [12]. However, the molecular mechanisms activating the Nlrp3 inflammasome in various cells and the relevance of this inflammasome activation is far from clear.

The Kawasaki disease model is characteristic of typical inflammatory cardiovascular diseases given its major pathological changes related to the inflammation in the walls of small- and medium-sized arteries, coronary arteries in particular [13]. *Lactobacillus casei* (*L. casei)* cell wall fragments (LCWE)-induced coronary arteritis is a well-established model that histopathologically mimics the coronary arteritis of Kawasaki disease [14, 15]. To date, the etiologic agent for Kawasaki disease is yet to be discovered, however, in LCWE model, typical pathological changes in coronary arteries are similar to those of Kawasaki disease patients including increased production of inflammatory cytokines in coronary arterial wall, infiltration of inflammatory cells, and aneurysm formation [16, 17]. Further, it has been shown that LCWE model of coronary arteritis is useful in duplicating or predicting human treatment responses because anti–TNF-α mAbs and intravenous gamma globulin were found to be effective in preventing coronary lesions in this model [14]. Therefore, it is of interest to investigate the molecular mechanisms for LCWE-induced cellular activation in the cardiovascular system. Here, we aim to investigate molecular activation of inflammasomes in endothelial cells by LCWE and address the implication of endothelial inflammasomes in the development of coronary arteritis.

In the present study, we first determined whether the Nlrp3 inflammasome is activated in response to LCWE in endothelial cells *in vivo* and *in vitro*. We then explored molecular mechanisms mediating Nlrp3 inflammasome activation by LCWE. Different possible pathways to activate this inflammasome were tested including lysosomal dysfunction and consequent release of cathepsin B, the effects of reactive oxygen species (ROS), and potassium channel-mediated membrane potassium movements. It is suggested that Nlrp3 inflammasome activation in coronary endothelial cells during LCWE stimulation may trigger and promote the endothelial dysfunction during coronary arteritis and that lysosomal stabilization is critical for the integrity of endothelial structure and function due to its action to inhibit inflammasome activation.

MATERIALS AND METHODS

Preparation of LCWE

The model of Kawasaki disease was prepared as previously described [14]. Briefly, *L. casei* bacteria (American Type Culture Collection, Manassas, VA) (ATCC 11578) were cultured in Lactobacillus MRS broth (BD Systems, USA) at 37 °C (on a shaker platform) and then harvested by centrifugation (10, 000 × g, 40 min) during the log phase of growth. After 6 washes with PBS (pH 7.2), *L. casei* bacteria were lysed by overnight incubation (at room temperature on a shaker platform) with 4 % SDS (Sigma-Aldrich, St. Louis, MO, USA) followed by 8 washes with PBS. The samples were then sequentially incubated with 250 μg/ml RNase, DNase I, and trypsin (Sigma-Aldrich, St. Louis, MO, USA) to remove any adherent material from the cell walls. Each of incubation was followed by 2 washes in PBS and then 4 washes only after the incubation with trypsin. After centrifugation, the pellet was sonicated (3 gram of packed wet weight in 9 ml of PBS) in a dry ice/ethanol bath for 2 h at a pulse setting of 5.0 (10-s pulse/5-s pause) (550 Sonic Dismembrator with a one-half-inch tapped horn and tapered microtip; one-eighth-inch diameter, tuned to vibrate at a fixed frequency of 20 KHz; Fisher Scientific, Nepean, Canada). Following 1-h centrifugation, the resultant supernatant containing the LCWE was harvested for treatment. The concentration of the preparation was detected by phenol-sulfuric acid colorimetric determination of the rhamnose content and expressed in mg/ml final concentration in PBS [16].

Animal procedures

C57BL/6J mice (4 weeks of age, male) were bred from breeding pairs from The Jackson Laboratory, Bar Harbor, ME, USA. All protocols were approved by the Institutional Animal Care and Use Committee of Virginia Commonwealth University. All mice were injected LCWE (i.p. 500 μg per mouse) to produce coronary arteritis as described in previous studies [14]. After 2 weeks, mice were sacrificed and heart tissues were harvested for immunohistochemistry and immunofluorescence examinations.

Cell culture

The mouse vascular endothelial cell (MVEC) line was purchased from ATCC (CRL-2586) and cultured as previously described[18]. The cell line was originally isolated from mouse hemangioendothelioma. MVECs were cultured in Dulbecco's modified Eagle's medium (DMEM) (Gibco, USA), containing 10 % of fetal bovine serum (Gibco, USA) and 1 %

penicillin–streptomycin (Gibco, USA). The cells were cultured in a humidified incubator at mixture at 37 °C with 5 % CO_2 and 95 % air. Cells were passaged by trypsinization (Trypsin/EDTA; Sigma, USA), followed by dilution in DMEM medium containing 10 % fetal bovine serum.

Immunohistochemistry

Hearts were embedded with paraffin, and 4 μm slices were cut from the embedded blocks. The tissue sections were stained with rabbit anti-VCAM-1 (1:50, Abcam, Cambridge, MA), anti-CD43 (1:50, Santa Cruz Biotech., CA), anti-F4/80 (1:50; AbD Serotec, Raleigh, NC), anti-Neutrophil marker (1:50, Santa Cruz Biotech., CA), and anti-IL1β (1:50, R&D systems, MN) overnight at 4 °C after a 20 min wash with 4 % H_2O_2 and 30 min blocking with 10% serum. Slides were incubated with primary antibodies diluted in phosphate-buffered saline (PBS) with 4 % serum. After incubation with each of these primary antibodies overnight, the sections were washed in PBS, incubated with biotinylated IgG (1:200) for 1 h, and then incubated with streptavidin-horseradish peroxidase for 30 min at room temperature. 50 μl of DAB were added to each section and stained for 1 min. After washing, the slides were counterstained with hematoxylin for 5 min. The slides were then mounted and observed under a microscope where photos were taken of the tissues. The area percentage of the endothelium positive for indicated staining in coronary arteries were analyzed by Image Pro Plus software (Media Cybernetics, Inc, Bethesda, MD).

Immunofluorescence microscopy

To confirm inflammasome activation in the endothelium of mouse coronary arteries, a FAM FLICA™ Caspase 1 Assay Kit (ImmunoChemistry Technologies, LLC, Bloomington, MN, USA) was used to detect active caspase-1 by FLICA probes. Frozen slides were fixed in acetone for 1 min then incubated overnight at 4°C with sheep anti-vWF antibody (1:200; Abcam, Cambridge, MA, USA) or anti-F4/80 (1:50; AbD Serotec, Raleigh, NC). Then, FLICA (1:10) and the fluorescence-conjugated secondary antibody were co-incubated for 1.5 hours at room temperature. Then, the slides were washed, mounted, and were visualized through sequentially scanning on an Olympus laser scanning confocal microscope (Fluoview FV1000, Olympus, Japan). For cell staining, MVECs grown on glass coverslips were treated as indicated and then fixed in 4 % PFA for 15 minutes. Cells were washed in phosphate-buffer saline (PBS) and incubated for 2 h at 4°C with indicated combination of goat anti-Nlrp3 (1:200, Abcam), rabbit anti-ASC (1:50, Santa Cruz Biotech.), or mouse anti-caspase-1 (1:100, Santa Cruz Biotech.) antibodies. Then cells were stained for another hour with fluorescence-conjugated secondary antibodies (1:500, Invitrogen) as indicated [19]. Then, slides were similarly process and visualized as above. Co-localization in coronary arteries or cells was analyzed by Image Pro Plus software, and the co-localization coefficient was represented by Pearson’s correlation coefficient.

Preparation of cytosolic fractions

Cells were washed twice with PBS and then homogenized in ice-cold HEPES buffer containing 20 mM HEPES, 255 mM sucrose, 1 mM EDTA, and 0.1 mM phenylmethylsulfony1 fluoride (pH 7.4). The supernatants (termed homogenates) containing

membrane and cytosolic fractions were obtained by centrifugation of samples at 1,000 × *g* for 10 min at 4 °C. A portion of homogenates was frozen in liquid N_2 and stored at −80 °C until use. Cytosolic fractions were prepared by a sequential centrifugation of the homogenates at 10,000 × *g* for 20 min and 100,000 × *g* for 90 min, as described previously [20].

Immunoblotting

Proteins from the MVECs were extracted using sucrose buffer (20 mM HEPES, 1mM EDTA, 255 mM sucrose, cocktail of protease inhibitors (Roche), pH 7.4. 20 μg protein samples were then denatured with 5× reducing Laemmli SDS-sample buffer and heated at 95 °C for 5 min. Samples were run on SDS-PAGE gel, transferred onto PVDF membrane and blocked. The membranes were then probed with primary antibody of either anti-caspase-1 (1:500, Santa Cruz Biotech) or anti-cathpesin B (1:500, Abcam) overnight at 4°C followed by incubation with horseradish peroxidase-labeled IgG (1:5000, Santa Cruz Biotech.). The immunoreactive bands were enhanced by chemiluminescence methods and imaged on Kodak Omat film. Densitometric analysis of the images obtained from X-ray films was performed using the Image J software (NIH).

Size-Exclusion Chromatography (SEC)

Proteins from MVECs were extracted from the homogenized cells with the following protein extraction buffer: 10 mM KCl, 20 mM 4-(2-hydroxyethyl)-1-piperazineethanesulfonic acid-KOH (pH 7.5), 1 mM EGTA, 1.5 mM EDTA and protease inhibitor cocktail (Roche). Samples were ultra-centrifuged at 18,000 × g for 10 min at 4°C, protein concentration of the supernatant was measured, and 1 mg of protein was run on a Superose 6 10/300 GL Column, with the following buffer: 50 mmol/L Tris (pH 7.4), 150 mmol/L NaCl, 1% octylglucoside, and 1 × protease inhibitor cocktail, connected to an ÄKTAprime plus chromatography system (GE Healthscience, Uppsala, Sweden). Fractions (600 μl) were collected starting at the void time and tested by western blot. 5 × loading buffer was added directly to the fractions, heated at 95 °C for 5 minutes, run on a SDS-polyacrylamide gel electrophoresis gels, and transferred to a PVDF membrane. After blocking, the membrane was probed with anti-caspase-1 (1:500) overnight at 4 °C, followed by incubation with horseradish peroxidase-labeled IgG (1:5000). The bands were detected, visualized and analyzed as described for Immunoblotting.

Nucleofection

Transfection of shRNA plasmids was performed using a 4D Nucleofector X-Unit (Lonza) according to the manufacturer's instructions. The GFP-Nlrp3 plasmid was obtained from Origene. Briefly, MVECs were tyrpsinized and centrifuged at 80 × g for 10 min. The cell pellet was resuspended in 100 μL SF Nucleofection solution (Lonza) for Nucleofection (with the program code DS198). This program was chosen based on the fact that Nucleofection efficiency was over 80% as analyzed by flow cytometry using control GFP plasmids. For each Nucleofection sample, 2 μg plasmid DNA was added in 100 μL P1 Nucleofection solution. After Nucleofection, cells were cultured in DMEM medium for 24 hours.

Analysis of lysosome membrane permeability

MVECs were cultured in eight-well chamber slides or 24-well culture plates and treated without or with LCWE for indicated time, or treated with glycyl-phenylalanine-2-naphthylamide, a lysosome-disrupting agent. Cells were then incubated with 1 μM acridine orange for 20 min at 37 °C, rinsed with PBS. Cells in chamber slides were immediately analyzed and photographed using a fluorescence microscope (Fluoview FV1000, Olympus, Japan). Cells in culture plates were analyzed for red-to-green fluorescence ratio of acridine orange staining by flow cytometry analysis using a flow cytometer (GUAVA, Hayward, CA, USA).

RNA interference of Cathepsin B

Small interference RNAs (siRNAs) for cathepsin B gene and scrambled small RNA were commercially available (Santa Cruz Biotechnology, CA). Transfection of siRNA was performed using the siLentFect Lipid Reagent (Bio-Rad, CA, USA) according to the manufacturer's instructions.

IL-1β production

After treatment, the cell supernatant was collected and IL-1β production was measured by a commercially available ELISA kit (R&D System, Minneapolis, MN) according to the protocol described by the manufacturer.

Statistics

Data are presented as means ± SE. Significant differences between and within multiple groups were examined using ANOVA for repeated measures followed by Duncan's multiple-range test. A student's t test was used to detect significant differences between two groups. The statistical analysis was performed using SigmaStat 3.5 software (Systat Software, San Jose, CA). $P < 0.05$ was considered statistically significant.

RESULTS

Increased vascular inflammation in coronary arteries in mice treated with LCWE

LCWE-induced coronary arteritis is a widely used mouse model for Kawasaki disease [14, 15]. VCAM-1 is a key molecule in mediating the adhesion of leukocytes including neutrophils, monocytes and lymphocytes, to vascular endothelium [21]. Increased expression of VCAM-1 has been considered as a marker for endothelial cell activation during vascular inflammation. As shown in Figure 1A, immunohistochemistry (IHC) studies demonstrated that treatment of mice with LCWE markedly increased the expression of VCAM-1 in the intima of coronary arteries. Such increase in VCAM-1 was further accompanied with increased adhesion of inflammatory cells including neutrophils (Figure 1B), T lymphocytes (Figure 1C), and macrophages (Figure 1D). It should be noted that in the present study, LCWE (500 μg per mouse) induced only mild lesion compared to more severe lesion reported in the literature. This discrepancy may be due to the difference in the purity of LCWE preparations. In our pilot experiments, we also found that LCWE at higher dose (1000 μg per mouse, 2 weeks) significantly increased mortality of mice (4 mice died of

6 mice, survival rate is only 33.33%), whereas no mice died when treated with 500 μg LCWE for 2 weeks. In the present study, we aimed to investigate whether and how endothelial inflammasome is activated during coronary arteritis. LCWE at this lower dose to induce coronary arteritis but not severe lesion is appropriate for this purpose.

Activation of endothelial inflammasomes in coronary arteries in mice treated with LCWE

Next, we examined whether endothelial activation and vascular inflammation are associated with activation of endothelial inflammasomes in coronary arteries of LCWE-treated mice. To this end, the activation of caspase-1 in the coronary arteries was detected by confocal microscopy using FLICA, a green fluorescent probe that specifically binds to the active form of caspase-1 protein. The endothelium was visualized by staining the coronary arteries with vWF, an endothelial cell marker. We detected a basal level of caspase1 activity (FLICA) in coronary endothelium (vWF) and found that 2-week LCWE (500 μg/mouse) treatment significantly increased the expression of active caspase-1 (FLICA) in the endothelium (vWF) as shown by increased co-localization coefficient between FLICA (green) and vWF (red) (Figure 2A). Consistently, the IHC studies demonstrated that the expression of IL-1β, an inflammasome product, was markedly enhanced in the intima of coronary arteries from LCWE-treated mice (Figure 2B). As shown in supplemnetary Fig. S1, an increased caspase1 activity can be detected in coronary endothelium of mice as early as 3 days after LCWE treatment. In constrast, increases in VCAM-1 expression occur at 7 days after LCWE treatment (supplemnetary Fig. S2). No changes in leukocyte adhesion were found even after 7 days of LCWE treatment (supplementary Fig. S3). Together, these data suggest that LCWE activate endothelial inflammasomes in coronary arteries *in vivo*, which is an earlier event compared to the formation of coronary arteritis.

Formation and activation of Nlrp3 inflammasome complex in MVECs upon LCWE stimulation

Nlrp3 inflammasome has been demonstrated as a principal machinery to trigger the inflammatory responses in a variety of mammalian cells including ECs [22]. We then determined whether LCWE induces Nlrp3 inflammasome formation and activation in ECs by analyzing the colocalization of Nlrp3 inflammasome components, the formation of high-molecular-weight protein complex consisting of Nlrp3 inflammasome oligomers, the cleavage of pro-caspase-1 to active caspase-1, and the production of IL-1β. As shown in Figure 3A–B, LCWE time-dependently increased the co-localization between Nlrp3 (green) and ASC (red) as shown by increased yellow staining and co-localization coefficient (maximal co-localization was observed after 8-hour LCWE stimulation). Similar increase in colocalization was found between Nlrp3 and caspase-1. Bryan *et al* have reported a marked redistribution of ASC from nuclei to cytol under inflammasome activation in macrophages[23], which is different from the ASC expression pattern in MVECs as we only observed a partial redistribution of ASC during inflammasome activation by LCWE and adipokine visfatin as described previously [18]. It is possible that ECs express a specific isoform which has different action than the isoform in macrophages [24].

The formation of functional Nlrp3 inflammasome requires the oligomerization of inflammasome monomers to form a high-molecular-weight protein complex, where pro-

caspase-1 proteins are cleaved to their active forms. To detect such formation of high-molecular-weight protein complex, we first performed size exclusion chromatography (SEC) to isolate proteins from MVECs into different fractions according to their size under the reduced condition and then detected the recruitment of pro-caspase-1 proteins in the high-molecular-weight fractions by Western blot. As shown in Figure 3C, we found that under resting control condition, pro-caspase-1 proteins were only detected in low-molecular-weight fractions, whereas markedly increase in pro-caspase-1 expression was observed in high-molecular-weight fractions when MVECs were treated with LCWE. Such shift of pro-caspase-1 from low-molecular-weight fractions into high-molecular-weight fractions indicates the formation of inflammasome complexes.

Consistent with the findings for the formation of Nlrp3 inflammasome complex, we further demonstrated that LCWE increased Nlrp3 inflammasome activity in MVECs as shown by enhanced cleavage of pro-caspase-1 proteins to their bio-active form (p20 subunit) (Figure 4A) and production of IL-1β production (Figure 4B), which peaked at 8 h after LCWE treatment. Such increase in inflammasome activation was completely abolished in cells transfected with Nlrp3 shRNA plasmids compared to those transfected with scramble shRNA plasmids (Figure 4C). Our data also demonstrated that LCWE induced Nlrp3 inflammasome formation and activation in human coronary arterial ECs as shown by increased the co-localization between Nlrp3 and caspase-1 or ASC and enhanced cleavage of pro-caspase-1 to active caspase-1 forms upon LCWE treatment (data not shown).

Activation of Nlrp3 inflammasomes by LCWE is associated with increased lysosome membrane permeability

Next, we investigated the molecular mechanism underlying LCWE-induced Nlrp3 inflammasome activation in MVECs. Previous studies have demonstrated three pathways to induce Nlrp3 inflammasome activation in mammalian cells including increased reactive oxygen species (ROS) production, potassium ions external flow, and lysosomal membrane permeabilization. We first examined the effects of N-acetyl-L-cysteine, an antioxidant that scavenges oxygen free radicals, and glibenclamide, a potassium channel blocker, on LCWE-induced caspase-1 activation and IL-1β production in MVECs. Both N-acetyl-L-cysteine and glibenclamide had no effects on either LCWE-induced caspase-1 activation (Figure 5A) or IL-1β production (Figure 5B) in MVECs. Thus, these results exclude the involvement of potassium ions external flow or ROS in LCWE-induced activation of Nlrp3 inflammasomes.

Previous studies have demonstrated that lysosomal membrane permeability is reduced by lysosome stabilization agents such as colchicine, ceramide, or dexamethasone [25–27]. Colchicine protects suspensions of lysososomes against spontaneous or induced disruption and has been termed lysosome “stabilizers” [25]. Ceramide-induced enhancement of fusion capacity may contribute to the Hsp70-mediated increase in lysosomal stability [27]. Dexamethasone megadoses may preserve lysosomal membrane integrity by a dual action involving both rapid nongenomic effects occurring instantaneously after administration and long-term receptor-dependent genomic events [26]. In the present study, we found that these lysosome membrane stabilizing agents blocked LCWE-induced formation of Nlrp3 inflammasomes (Figure 6A–B), activation of caspase-1 (Figure 6C), and production of

IL-1β (Figure 6D) in MVECs. Taken together, these data suggest that increased lysosome membrane permeabilization is involved in LCWE-induced Nlrp3 inflammasome formation and activation in MVECs.

Increased lysosome membrane permeability and cathepsin B release in MVECs by LCWE

To directly monitor the changes in lysosome membrane permeability in live MVECs, cells were stained with the lysomotropic agent acridine orange which accumulates in acidic organelles such as lysosomes with red fluorescence and shows green fluorescence in neutral environment such as cytoplasm and nucleus [28]. Increased lysosome membrane permeability causes lysosomal alkalization resulting in decreased red fluorescence for acridine orange. As shown in Figure 7A, lysosomes in control cells were visualized as red puncta with high fluorescent intensity, while LCWE treatment time-dependently decreased the number and fluorescence intensity of red puncta. Quantification of red-to-green fluorescence ratio by flow cytometry (Figure 7B) further indicated that a maximal decrease by LCWE was observed at 8 hour of LCWE stimulation, which was similar to the effect of glycyl-L-phenylalanine 2-naphthylamide (GPN), a tripeptide causing osmotic lysis of lysosomes. Lysosomal release of cathepsin B has been shown to play a crucial role in mediating Nlrp3 inflammasome activation induced by lysosome membrane permeabilization [29, 30]. As shown in Figure 7C, we also found a marked increase in cathepsin B expression in the cytosol of MVECs upon LCWE stimulation suggesting that cathepsin B release may be a consequence of increased lysosome membrane permeability leading to Nlrp3 inflammasome activation.

Effects of cathepsin B gene silencing on LCWE-induced Nlrp3 inflammasome activation *in vitro*

We further showed that inhibition of cathepsin B activity in MVECs by silencing cathepsin B genes markedly inhibited LCWE-induced colocalization of Nlrp3 with caspase-1 (Figure 8A), cleavage of pro-caspase-1 (Figure 8B), and production of IL-1β (Figure 8C). It was confirmed that cathespsin B gene silencing by cathepsin B siRNA transfection could efficiently knockdown the cathepsin B protein expression by 78% (Figure 8D). These findings further indicate that cathepsin B is involved in LCWE-induced Nlrp3 inflammasome activation in MVECs.

Effects of cathepsin B inhibition on LCWE-induced Nlrp3 inflammasome activation *in vivo*

Previous study have reported that cathepsin B inhibitor Ca-074Me could block Nlrp3 inflammasome-mediated inflammatory responses *in vivo* [31]. Similarly, we found that treatment of mice with Ca-074Me abolished LCWE-induced inflammasome activation in coronary artierial endothelium (Figure 9A–B). These findings confirm that cathepsin B is involved in LCWE-induced endothelial Nlrp3 inflammasome activation *in vivo*. Furthermore, treatment of mice with Ca-074Me markedly blocked LCWE-induced increases in adhesion of inflammatory cells including macrophages (Fig. 9C–D) and neutrophils (Fig. 9E–F). As shown in supplementary Fig. S2, Ca-074Me also abolished LCWE-induced VCAM-1 expression in coronary endothelium. These data suggest that inhibition of cathepsin B also blocks LCWE-induced coronary arteritis.

DISCUSSION

The present study demonstrated that endothelial Nlrp3 inflammasomes were formed and activated both *in vivo* and *in vitro* upon stimulation with LCWE, a bacterial extract that is widely used to induce coronary arteritis in mice. Such action of LCWE on Nlrp3 inflammasomes in endothelial cells was associated with increased lysosomal membrane permeability and cathepsin B release.

Using an established mouse model of Kawasaki disease that involves injection of LCWE, recent studies have implicated that Nlrp3 inflammasome is a major intracellular molecular machinery to switch on the inflammatory responses that contribute to the development of coronary arteritis and lesions leading to atherosclerotic acceleration [14, 15, 32]. It was demonstrated that LCWE-induced IL-1β maturation and secretion was dependent on the Nlrp3 inflammasome in macrophages and both caspase1-deficient and IL-1 receptor-deficient mice were protected from LCWE-induced coronary lesions [14]. LCWE treatment of both $ApoE^{-/-}$ and $Ldlr^{-/-}$ mice on the high fat diet, two widely used genetic mouse models for atherosclerosis, dramatically accelerated atherosclerosis in these mice with increases in en face aortic atherosclerosis and plaque size in both the aortic sinuses and arch plaques [32]. These previous studies have elegantly demonstrated an essential role of Nlrp3 inflammasome in mediating the inflammatory response by macrophages, however, it remains unknown about the actions of Nlrp3 inflammasomes in vascular cell dysfunction or injury such as endothelial dysfunction, which has been suggested to the earliest step in the development of coronary arteritis as well as atherosclerosis. [33–35]. In the present study, we first demonstrated that LCWE-induced coronary arteritis in a mouse model for Kawasaki disease was sucessfuly developed as shown by enhanced endothelial expression of VCAM-1 and increased adhesion of leukocytes to the coronary arterial walls (Fig. 1). These pathological findings of LCWE-treated mice also resembled those of human coronary artery lesions in acute-phase Kawasaki disease patients, which showed infiltration of neutrophils, macrophages and lymphocytes at early stages [36]. Up-regulation of VCAM-1 has been considered as one of early markers for endothelial cell activation and dysfunction, which occurs at the early developmental stage of various cardiovascular diseases such as atherosclerosis [37–39]. Inhibiting the function of VCAM-1 blocks leukocyte recruitment and thus tissue in ammation in atherosclerosis [37]. More importantly, our data demonstrated that the changes in VCAM-1 and leukocyte adhesion ability of endothelial cells were correlated with enhanced Nlrp3 inflammasome activity in the coronary endothelium (Fig. 2). Thus, these findings support the view that activation of endothelial Nlrp3 inflammasomes may represent an important mechanism that causes endothelial dysfunction leading to exaggerated inflammatory responses in coronary arteries by recruitment of inflammatory cells which ultimately contributing to the development of coronary arteritis and lesions.

By various approaches, we confirmed that LCWE stimulation induced the formation and activation of the Nlrp3 inflammasome complex in cultured endothelial cells, as shown by colocalization of Nlrp3 with ASC or caspase-1 using confocal microscopy, by an increase in recruitment of pro-caspase-1 to the large molecular fractions detected by SEC and by biochemical analysis of caspase-1 activity and production of IL-1β. These results clearly

suggest that the Nlrp3 inflammasomes are functioning in endothelial cells and that LCWE stimulation can lead to its activation. Our results are consistent with previous findings showing that Nlrp3 inflammasome, first characterized in immune cells, can be also detected in various non-immune cells such as endothelial cells and other residential cells in the brain, heart, and vessels [40]. Although there are some reports that Nlrp3 inflammasomes can be activated in endothelial cells under different pathological conditions such as shear stress, hemorrhagic shock, and diet-induced dyslipidemia [22, 41, 42], the results from the present study provide the first experimental evidence that LCWE activates Nlrp3 inflammasomes in endothelial cells, which may be an important pathogenic mechanism responsible for endothelial dysfunction in the context of coronary arteritis.

Another important finding of the present study is that LCWE-induced Nlrp3 inflammasome activation is primarily through lysosomal destabilization-mediated signaling pathway. Previous studies have demonstrated that activation of Nlrp3 inflammasomes proceeds through at least three mutually non-exclusive mechanisms, including the K^+ efflux, generation of reactive oxygen species, and lysosome membrane permeabilization pathway [9, 43, 44]. In the present study, we demonstrated that LCWE-induced endothelial Nlrp3 inflammasome activation was independent of K^+ channel activity and ROS production as shown by ineffectiveness of potassium channel blocker glibenclamdie or ROS scavenger N-acetyl-L-cysteine on LCWE-induced caspase-1 activation and IL-1β production. In contrast, LCWE-induced increases in Nlrp3 inflammasome formation and functionality were markedly attenuated by three mechanistically distinct lysosome stabilization agents, namely colchicine, dexamethasone, and ceramide. Although these agents have been claimed as lysosome stabilizers, it should be noted that none of them is specific for lysosome stabilization [25–27]. Nonetheless, our data from these mechanistically distinct stabilizers implicate that lysosome stability controls the Nlrp3 inflammasome activation and functionality in response to LCWE. Interestingly, recent studies have demonstrated that hemorrhagic shock or shear stress increases NADPH oxidase-derived ROS, which promote the association of thioredoxin-interacting protein with the Nlrp3 protein and subsequently induce inflammasome activation in endothelial cells [22, 41]. The discrepancy between these previous findings and our results for inflammasome activation is unclear. It appears that Nlrp3 inflammasome machinery in endothelial cells can be instigated via distinct mechanisms depending on the types of stimuli or pathological conditions.

Lysosome destabilization results the release of cathepsin B, a lysosomal hydrolase that induces Nlrp3 inflammasome in a number of immune cells [45–47]. By monitoring the accumulation of lysomotropic dye acridinge orange, the present study provided the first direct evidence that LCWE disrupted lysosomal integrity and a release of lysosomal cathepsin B into the cytosol. We also blocked cathepsin B function by silencing its gene and observed that endothelial cells transfected with cathepsin B siRNA showed much less inflammasome formation and functionality. Lastly, treatment of mice with cathepsin B inhibitor Ca-074Me abolished LCWE-induced endothelial inflammasome activation in coronary arteries suggesting that inhibition of cathepsin B also blocks LCWE-induced Nlrp3 activation in endothelial cells *in vivo*. Thus, our *in vitro* and *in vivo* data confirm the role of lysosome destabilization-cathepsin B signaling pathway in inducing Nlrp3 inflammasome in

endothelial cells upon LCWE stimulation. The present study did not attempt to define the mechanism how LCWE induce lysosome destabilization-cathepsin B pathway. LCWE are mainly composed of polysaccharides and it has been reported that lipopolysaccharides from *Escherichia coli* or *Porphyromonas gingivalis* up-regulate the lysosomal-cathepsin B-dependent signaling in endothelial cells [48, 49]. Thus, the effect of LCWE on endothelial cells may resemble those of lipopolysaccharides due to their similarity in chemical structures. Furthermore, inhibition of cathepsin B blocks LCWE-induced coronary arteritis since treatment of mice with Ca-074Me markedly blocked LCWE-induced increases in VCAM-1 expression (supplementary Fig. S2) and adhesion of inflammatory cells including macrophages and neutrophils (Fig. 9C-F). These data imply that lysosomal-cathepsin B-dependent inflammasome activation could be a therapeutical target for coronary arteritis and consequent lesions.

Our *in vitro* and *in vivo* data suggest that activation of endothelial inflammasome by LCWE is associated with endothelial dysfunction and increased adhesion ability during LCWE-induced coronary arteritis. However, our *in vivo* data did not rule out a role of inflammasomes in other cell types such as macrophages in LCWE-induced arteritis. This is in line with previous findings that the pathogenesis of LCWE-induced coronary arteritis is complex and has also been attributed to the functions of other inflammatory cells such T cells [50] and monocytes [51]. The present study did not attempt to dissect the role of endothelial inflammasomes from the ones in other cell types. The implementation of such goal would require tissue-specific knockout animal models (*e.g.* endothelial cell-deleted Nlrp3 mouse model) in the future studies. Nonetheless, our data support the view that endothelial inflammasome activation may serve as a contributing mechanism that initiates or exacerbates the development of coronary arteritis and lesion.

In summary, the present study demonstrated that in a LCWE-treated mouse model of coronary arteritis, endothelial dysfunction associated with increased adhesion ability is correlated with the formation and activation of Nlrp3 inflammasomes in the coronary endothelium. Such activation of endothelial Nlrp3 inflammasome by LCWE is due to lysosome membrane permeabilization and cathepsin B release and can be suppressed by lysosome stabilization agents. Our results provide new mechanistic insights into understanding the molecular activation of the inflammasome in endothelial cells and its role in endothelial dysfunction leading to vascular inflammation, which may ultimately contribute to the development of coronary arteritis and lesion.

Supplementary Material

Refer to Web version on PubMed Central for supplementary material.

Acknowledgments

This study was supported by grants from the National Institute of Health (HL057244, HL075316 and HL091464 to PL; HL122937 and HL122769 to YZ).

References

1. Menu P, Pellegrin M, Aubert JF, Bouzourene K, Tardivel A, Mazzolai L, Tschopp J. Atherosclerosis in ApoE-deficient mice progresses independently of the NLRP3 inflammasome. Cell Death Dis. 2011; 2:e137. [PubMed: 21451572]
2. Abais JM, Zhang C, Xia M, Liu Q, Gehr TW, Boini KM, Li PL. NADPH oxidase-mediated triggering of inflammasome activation in mouse podocytes and glomeruli during hyperhomocysteinemia. Antioxid Redox Signal. 2013; 18:1537–1548. [PubMed: 23088210]
3. Zhang C, Boini KM, Xia M, Abais JM, Li X, Liu Q, Li PL. Activation of Nod-like receptor protein 3 inflammasomes turns on podocyte injury and glomerular sclerosis in hyperhomocysteinemia. Hypertension. 2012; 60:154–162. [PubMed: 22647887]
4. Martinon F, Burns K, Tschopp J. The inflammasome: a molecular platform triggering activation of inflammatory caspases and processing of proIL-beta. Mol Cell. 2002; 10:417–426. [PubMed: 12191486]
5. Lamkanfi M, Malireddi RK, Kanneganti TD. Fungal zymosan and mannan activate the cryopyrin inflammasome. J Biol Chem. 2009; 284:20574–20581. [PubMed: 19509280]
6. Kanneganti TD, Body-Malapel M, Amer A, Park JH, Whitfield J, Franchi L, Taraporewala ZF, Miller D, Patton JT, Inohara N, Nunez G. Critical role for Cryopyrin/Nalp3 in activation of caspase-1 in response to viral infection and double-stranded RNA. J Biol Chem. 2006; 281:36560–36568. [PubMed: 17008311]
7. Kepp O, Galluzzi L, Zitvogel L, Kroemer G. Pyroptosis - a cell death modality of its kind? Eur J Immunol. 2010; 40:627–630. [PubMed: 20201017]
8. De Nardo D, Latz E. NLRP3 inflammasomes link inflammation and metabolic disease. Trends Immunol. 2011; 32:373–379. [PubMed: 21733753]
9. Lamkanfi M. Emerging inflammasome effector mechanisms. Nat Rev Immunol. 2011; 11:213–220. [PubMed: 21350580]
10. Nicolson GL, Ash ME. Lipid Replacement Therapy: A natural medicine approach to replacing damaged lipids in cellular membranes and organelles and restoring function. Biochim Biophys Acta. 2013
11. Misawa T, Takahama M, Kozaki T, Lee H, Zou J, Saitoh T, Akira S. Microtubule-driven spatial arrangement of mitochondria promotes activation of the NLRP3 inflammasome. Nat Immunol. 2013; 14:454–460. [PubMed: 23502856]
12. Gattorno M, Martini A. Beyond the NLRP3 inflammasome: autoinflammatory diseases reach adolescence. Arthritis Rheum. 2013; 65:1137–1147. [PubMed: 23400910]
13. Scuccimarri R. Kawasaki disease. Pediatr Clin North Am. 2012; 59:425–445. [PubMed: 22560578]
14. Lee Y, Schulte DJ, Shimada K, Chen S, Crother TR, Chiba N, Fishbein MC, Lehman TJ, Arditi M. Interleukin-1beta is crucial for the induction of coronary artery inflammation in a mouse model of Kawasaki disease. Circulation. 2012; 125:1542–1550. [PubMed: 22361326]
15. Tomita S, Myones BL, Shulman ST. In vitro correlates of the L. casei animal model of Kawasaki disease. J Rheumatol. 1993; 20:362–367. [PubMed: 8097251]
16. Lehman TJ, Walker SM, Mahnovski V, McCurdy D. Coronary arteritis in mice following the systemic injection of group B Lactobacillus casei cell walls in aqueous suspension. Arthritis Rheum. 1985; 28:652–659. [PubMed: 3924060]
17. Lehman TJ, Warren R, Gietl D, Mahnovski V, Prescott M. Variable expression of Lactobacillus casei cell wall-induced coronary arteritis: an animal model of Kawasaki's disease in selected inbred mouse strains. Clin Immunol Immunopathol. 1988; 48:108–118. [PubMed: 3133145]
18. Xia M, Boini KM, Abais JM, Xu M, Zhang Y, Li PL. Endothelial NLRP3 Inflammasome Activation and Enhanced Neointima Formation in Mice by Adipokine Visfatin. Am J Pathol. 2014; 184:1617–1628. [PubMed: 24631027]
19. Xia M, Zhang C, Boini KM, Thacker AM, Li PL. Membrane raft-lysosome redox signalling platforms in coronary endothelial dysfunction induced by adipokine visfatin. Cardiovasc Res. 2011; 89:401–409. [PubMed: 20823276]

20. Zhang DX, Fryer RM, Hsu AK, Zou AP, Gross GJ, Campbell WB, Li PL. Production and metabolism of ceramide in normal and ischemic-reperfused myocardium of rats. Basic Res Cardiol. 2001; 96:267–274. [PubMed: 11403420]
21. Mayet WJ, Schwarting A, Orth T, Duchmann R, Meyer zum Buschenfelde KH. Antibodies to proteinase 3 mediate expression of vascular cell adhesion molecule-1 (VCAM-1). Clin Exp Immunol. 1996; 103:259–267. [PubMed: 8565309]
22. Xiao H, Lu M, Lin TY, Chen Z, Chen G, Wang WC, Marin T, Shentu TP, Wen L, Gongol B, Sun W, Liang X, Chen J, Huang HD, Pedra JH, Johnson DA, Shyy JY. Sterol regulatory element binding protein 2 activation of NLRP3 inflammasome in endothelium mediates hemodynamic-induced atherosclerosis susceptibility. Circulation. 2013; 128:632–642. [PubMed: 23838163]
23. Bryan NB, Dorfleutner A, Rojanasakul Y, Stehlik C. Activation of inflammasomes requires intracellular redistribution of the apoptotic speck-like protein containing a caspase recruitment domain. J Immunol. 2009; 182:3173–3182. [PubMed: 19234215]
24. Bryan NB, Dorfleutner A, Kramer SJ, Yun C, Rojanasakul Y, Stehlik C. Differential splicing of the apoptosis-associated speck like protein containing a caspase recruitment domain (ASC) regulates inflammasomes. J Inflamm (Lond). 2010; 7:23. [PubMed: 20482797]
25. Nuki G. Colchicine: its mechanism of action and efficacy in crystal-induced inflammation. Curr Rheumatol Rep. 2008; 10:218–227. [PubMed: 18638431]
26. Hinz B, Hirschelmann R. Dexamethasone megadoses stabilize rat liver lysosomal membranes by non-genomic and genomic effects. Pharm Res. 2000; 17:1489–1493. [PubMed: 11303958]
27. Kirkegaard T, Roth AG, Petersen NH, Mahalka AK, Olsen OD, Moilanen I, Zylicz A, Knudsen J, Sandhoff K, Arenz C, Kinnunen PK, Nylandsted J, Jaattela M. Hsp70 stabilizes lysosomes and reverts Niemann-Pick disease-associated lysosomal pathology. Nature. 2010; 463:549–553. [PubMed: 20111001]
28. Granato M, Lacconi V, Peddis M, Lotti LV, Renzo LD, Gonnella R, Santarelli R, Trivedi P, Frati L, D'Orazi G, Faggioni A, Cirone M. HSP70 inhibition by 2-phenylethynesulfonamide induces lysosomal cathepsin D release and immunogenic cell death in primary effusion lymphoma. Cell Death Dis. 2013; 4:e730. [PubMed: 23868063]
29. Martinon F, Petrilli V, Mayor A, Tardivel A, Tschopp J. Gout-associated uric acid crystals activate the NALP3 inflammasome. Nature. 2006; 440:237–241. [PubMed: 16407889]
30. Hornung V, Bauernfeind F, Halle A, Samstad EO, Kono H, Rock KL, Fitzgerald KA, Latz E. Silica crystals and aluminum salts activate the NALP3 inflammasome through phagosomal destabilization. Nat Immunol. 2008; 9:847–856. [PubMed: 18604214]
31. Hoegen T, Tremel N, Klein M, Angele B, Wagner H, Kirschning C, Pfister HW, Fontana A, Hammerschmidt S, Koedel U. The NLRP3 inflammasome contributes to brain injury in pneumococcal meningitis and is activated through ATP-dependent lysosomal cathepsin B release. J Immunol. 2011; 187:5440–5451. [PubMed: 22003197]
32. Chen S, Lee Y, Crother TR, Fishbein M, Zhang W, Yilmaz A, Shimada K, Schulte DJ, Lehman TJ, Shah PK, Arditi M. Marked acceleration of atherosclerosis after Lactobacillus casei-induced coronary arteritis in a mouse model of Kawasaki disease. Arterioscler Thromb Vasc Biol. 2012; 32:e60–71. [PubMed: 22628430]
33. Nakatani K, Takeshita S, Tsujimoto H, Kawamura Y, Tokutomi T, Sekine I. Circulating endothelial cells in Kawasaki disease. Clin Exp Immunol. 2003; 131:536–540. [PubMed: 12605708]
34. Fukazawa R, Ikegam E, Watanabe M, Hajikano M, Kamisago M, Katsube Y, Yamauchi H, Ochi M, Ogawa S. Coronary artery aneurysm induced by Kawasaki disease in children show features typical senescence. Circ J. 2007; 71:709–715. [PubMed: 17456996]
35. Yu X, Hirono KI, Ichida F, Uese K, Rui C, Watanabe S, Watanabe K, Hashimoto I, Kumada T, Okada E, Terai M, Suzuki A, Miyawaki T. Enhanced iNOS expression in leukocytes and circulating endothelial cells is associated with the progression of coronary artery lesions in acute Kawasaki disease. Pediatr Res. 2004; 55:688–694. [PubMed: 14764920]
36. Takahashi K, Oharaseki T, Naoe S, Wakayama M, Yokouchi Y. Neutrophilic involvement in the damage to coronary arteries in acute stage of Kawasaki disease. Pediatr Int. 2005; 47:305–310. [PubMed: 15910456]

37. Kaufmann BA, Sanders JM, Davis C, Xie A, Aldred P, Sarembock IJ, Lindner JR. Molecular imaging of inflammation in atherosclerosis with targeted ultrasound detection of vascular cell adhesion molecule-1. Circulation. 2007; 116:276–284. [PubMed: 17592078]

38. Cines DB, Pollak ES, Buck CA, Loscalzo J, Zimmerman GA, McEver RP, Pober JS, Wick TM, Konkle BA, Schwartz BS, Barnathan ES, McCrae KR, Hug BA, Schmidt AM, Stern DM. Endothelial cells in physiology and in the pathophysiology of vascular disorders. Blood. 1998; 91:3527–3561. [PubMed: 9572988]

39. Kaufmann BA, Carr CL, Belcik JT, Xie A, Yue Q, Chadderdon S, Caplan ES, Khangura J, Bullens S, Bunting S, Lindner JR. Molecular imaging of the initial inflammatory response in atherosclerosis: implications for early detection of disease. Arterioscler Thromb Vasc Biol. 2010; 30:54–59. [PubMed: 19834105]

40. Ramaswamy V, Walsh JG, Sinclair DB, Johnson E, Tang-Wai R, Wheatley BM, Branton W, Maingat F, Snyder T, Gross DW, Power C. Inflammasome induction in Rasmussen's encephalitis: cortical and associated white matter pathogenesis. J Neuroinflammation. 2013; 10:152. [PubMed: 24330827]

41. Xiang M, Shi X, Li Y, Xu J, Yin L, Xiao G, Scott MJ, Billiar TR, Wilson MA, Fan J. Hemorrhagic shock activation of NLRP3 inflammasome in lung endothelial cells. J Immunol. 2011; 187:4809–4817. [PubMed: 21940680]

42. Mohamed IN, Hafez SS, Fairaq A, Ergul A, Imig JD, El-Remessy AB. Thioredoxin-interacting protein is required for endothelial NLRP3 inflammasome activation and cell death in a rat model of high-fat diet. Diabetologia. 2013

43. Zhou R, Yazdi AS, Menu P, Tschopp J. A role for mitochondria in NLRP3 inflammasome activation. Nature. 2011; 469:221–225. [PubMed: 21124315]

44. Mariathasan S, Weiss DS, Newton K, McBride J, O'Rourke K, Roose-Girma M, Lee WP, Weinrauch Y, Monack DM, Dixit VM. Cryopyrin activates the inflammasome in response to toxins and ATP. Nature. 2006; 440:228–232. [PubMed: 16407890]

45. Jin C, Flavell RA. Molecular mechanism of NLRP3 inflammasome activation. J Clin Immunol. 2010; 30:628–631. [PubMed: 20589420]

46. Duewell P, Kono H, Rayner KJ, Sirois CM, Vladimer G, Bauernfeind FG, Abela GS, Franchi L, Nunez G, Schnurr M, Espevik T, Lien E, Fitzgerald KA, Rock KL, Moore KJ, Wright SD, Hornung V, Latz E. NLRP3 inflammasomes are required for atherogenesis and activated by cholesterol crystals. Nature. 2010; 464:1357–1361. [PubMed: 20428172]

47. Goncalves VM, Matteucci KC, Buzzo CL, Miollo BH, Ferrante D, Torrecilhas AC, Rodrigues MM, Alvarez JM, Bortoluci KR. NLRP3 controls Trypanosoma cruzi infection through a caspase-1-dependent IL-1R-independent NO production. PLoS Negl Trop Dis. 2013; 7:e2469. [PubMed: 24098823]

48. Li JH, D'Alessio A, Pober JS. Lipopolysaccharide can trigger a cathepsin B-dependent programmed death response in human endothelial cells. Am J Pathol. 2009; 175:1124–1135. [PubMed: 19661440]

49. Huck O, Elkaim R, Davideau JL, Tenenbaum H. Porphyromonas gingivalis and its lipopolysaccharide differentially regulate the expression of cathepsin B in endothelial cells. Mol Oral Microbiol. 2012; 27:137–148. [PubMed: 22520384]

50. Duong TT, Silverman ED, Bissessar MV, Yeung RS. Superantigenic activity is responsible for induction of coronary arteritis in mice: an animal model of Kawasaki disease. Int Immunol. 2003; 15:79–89. [PubMed: 12502728]

51. Lin IC, Kuo HC, Lin YJ, Wang FS, Wang L, Huang SC, Chien SJ, Huang CF, Wang CL, Yu HR, Chen RF, Yang KD. Augmented TLR2 expression on monocytes in both human Kawasaki disease and a mouse model of coronary arteritis. PLoS One. 2012; 7:e38635. [PubMed: 22737215]

Highlights

- Endothelial inflammasome is activated during coronary arteritis in mice treated with LCWE
- LCWE activates endothelial Nlrp3 inflammasomes via lysosome permeabilization and cathepsin B.
- Activation of endothelial Nlrp3 inflammasomes is suppressed by lysosome stabilizing agents.

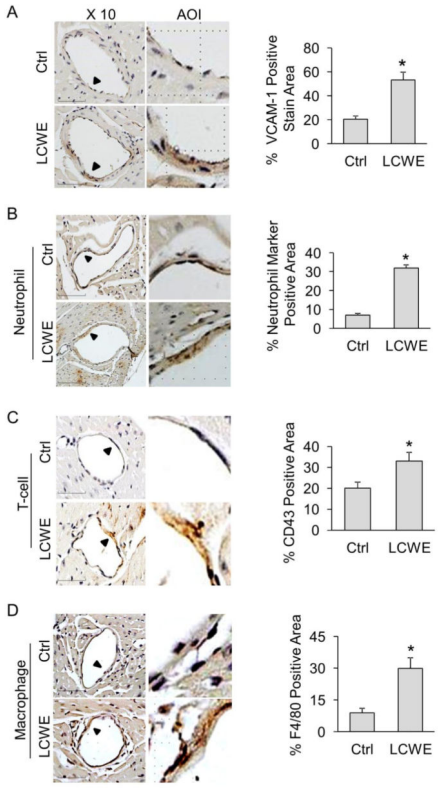

Fig. 1. Increased VCAM-1 expression and leukocyte adhesion in coronary arterial endothelium of mice treated with LCWE

Mice were intraperitoneally treated with either saline control (Ctrl) or LCWE (500 μg, 2 weeks). (A) IHC staining showing the expression of VCAM-1 in the endothelium of coronary arteries. Summarized data showing area percentage of the endothelium positive for VCAM-1 staining in coronary arteries. (B) IHC staining showing the expression of neutrophil marker in the endothelium of coronary arteries. Summarized data showing area percentage of the endothelium positive for neutrophil marker in coronary arteries. (C) IHC staining showing the expression of T cell marker CD43 in the endothelium of coronary arteries. Summarized data showing area percentage of the endothelium positive for CD43 in coronary arteries. (D) IHC staining showing the expression of macrophage marker F4/80 in the endothelium of coronary arteries. Summarized data showing area percentage of the endothelium positive for F4/80 in coronary arteries. Enlarged images of area of interest (AOI) are indicated with an arrow. Scale bar: 50 μm. N = 6 mice per group. *$P < 0.05$ *vs.* LCWE on WT.

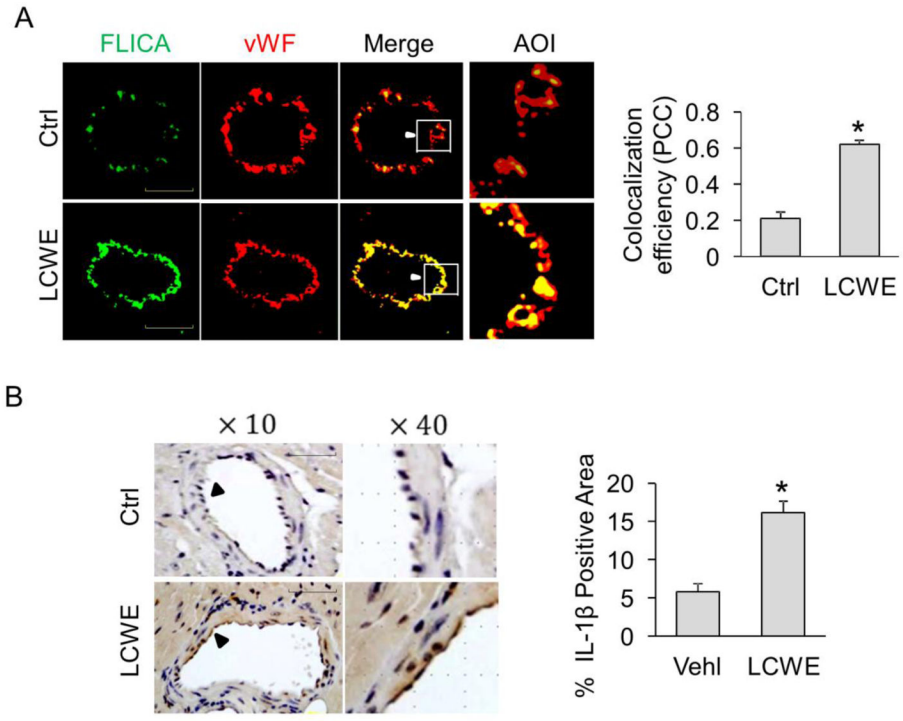

Fig. 2. Activation of endothelial inflammasomes in coronary arteries of mice treated with LCWE

Mice were intraperitoneally treated with saline control (Ctrl) or LCWE (500 μg, 2 weeks). (A) Frozen sections of mouse hearts were stained with FLICA, a green fluorescent probe specific for active caspase-1, and Alexa555-conjugated antibodies against an endothelial cell marker vWF in coronary arteries. The merged images displayed yellow dots or patches indicating the colocalization of FLICA (green) with vWF (red). Summarized data showing the colocalization coefficient of FLICA with vWF (n = 5). (B) IHC staining showing the expression of IL-1β in the endothelium of coronary arteries. Summarized data showing area percentage of the endothelium positive for IL-1β in coronary arteries. High-power magnification of AOI is indicated with an arrow. Scale bar = 50 μm. n = 6 mice per group. *P < 0.05 vs. control.

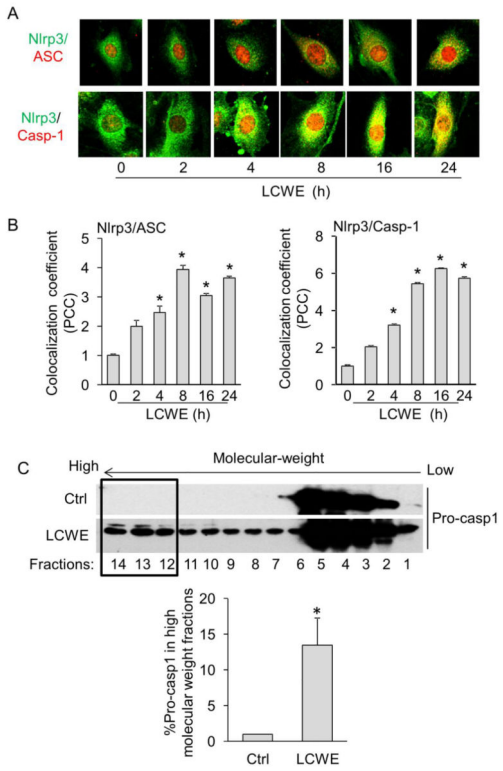

Fig. 3. Formation of Nlrp3 inflammasome in MVECs upon LCWE stimulation

(A, B) MVECs were stained with Alexa488-conjugated anti-Nlrp3 and Alexa555-conjugated anti-ASC or anti-caspase1 antibodies. Representative images in panel A show the colocalization (yellow) of Nlrp3 (green) with ASC (red) or Nlrp3 (green) with caspase-1 (red) under stimulation of LCWE (10 μg/ml) for 0–24 hours. Summarized data in panel B show the colocalization coefficiency of Nlrp3 with ASC or Nlrp3 with caspase-1 (n = 5). * $P < 0.05$ vs. LCWE 0 h. (C) MVECs were stimulated without (Ctrl) or with LCWE (10 μg/ml) for different time points (2, 4, 8, 16, and 24 hours) and then lysed. Cell lysates were used for size-exclusion chromatography (SEC) followed by Western blot analysis of eluted fractions using antibodies against pro-caspase-1. Summarized data show the percentage of pro-caspase-1 expression in the high molecular weight fractions (#12–14) compared to total expression of pro-caspase-1 (#1–14) (n = 3). * $P < 0.05$ vs. Ctrl.

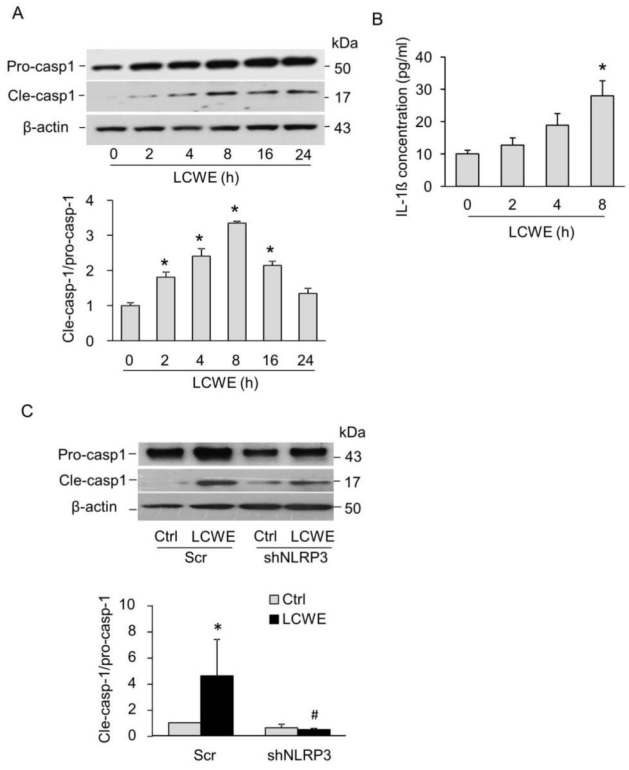

Fig. 4. LCWE increased Nlrp3 inflammasome activity in MVECs

(A) Representative immunoblotting documents and summarized data showing the effects of LCWE (10 μg/ml for 0–24 hours) on the expression of pro-caspase-1, cleaved caspase-1 and β-actin in MVECs (n = 4). * $P < 0.05$ *vs.* LCWE 0 h. (B) Effects of LCWE (10 μg/ml for 0–8 hour) on IL-1β production in MVECs (n = 6) * $P < 0.05$ *vs.* LCWE 0 h. (C) Representative Western blot documents and summarized data showing the effect of LCWE (10 μg/ml, 8 h) on the expression of pro-caspase-1, cleaved caspase-1 and β-actin expression in MVECs transfected with scrambled shRNA (Scr) or Nlrp3 shRNA plasmids (n = 4). * $P < 0.05$ vs. scrambled control; # $P < 0.05$ *vs.* scramble+LCWE.

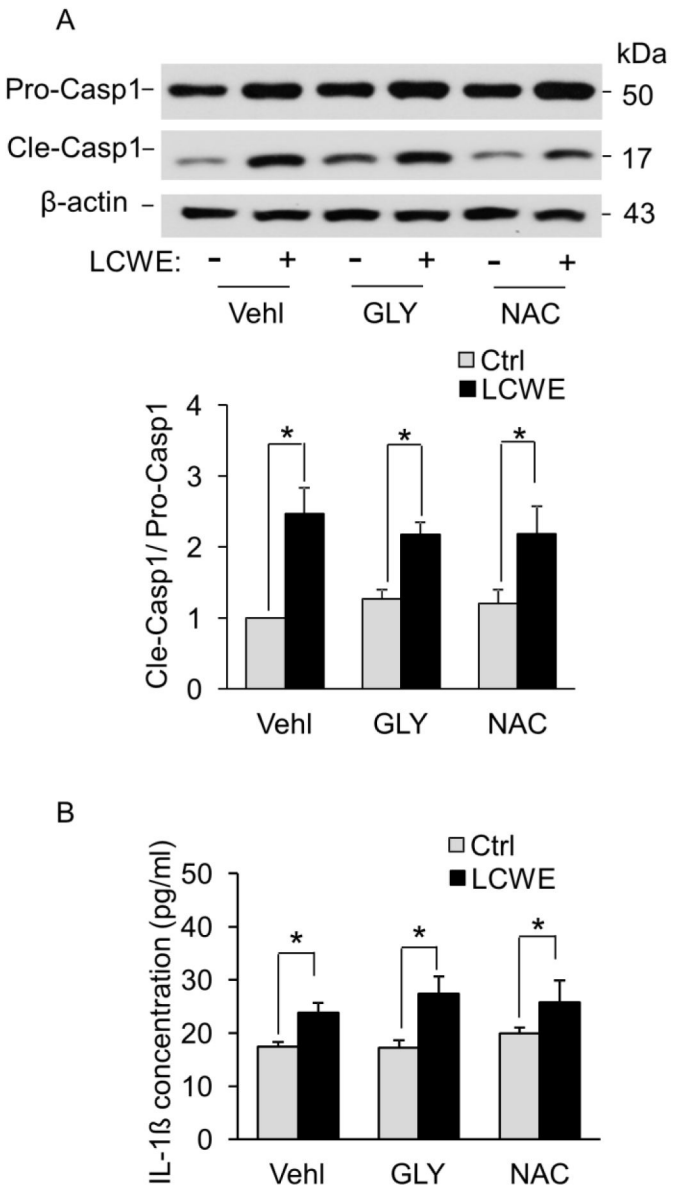

Fig. 5. Effects of potassium channel blockade or ROS scavenging on LCWE-induced activation of Nlrp3 inflammasomes in MVECs

MVECs were stimulated with or without LCWE (10 μg/ml, 8 h) in the presence of PBS (Vehl: vehicle), potassium channel blocker glibenclamide (GLY, 10 μM, Sigma) or ROS scavenger N-acetyl-L-cysteine (NAC, 10 μM, Sigma). (A) Representative Western blot documents and summarized data showing the effects of glibenclamide or N-acetyl-L-cysteine on the expression of pro-caspase-1, cleaved caspase-1 and β-actin (n = 3). (B) IL-1β production measurement in MVECs by ELISA (n=6). * $P < 0.05$, LCWE vs. control; # $P < 0.05$ *vs.* vehicle+LCWE.

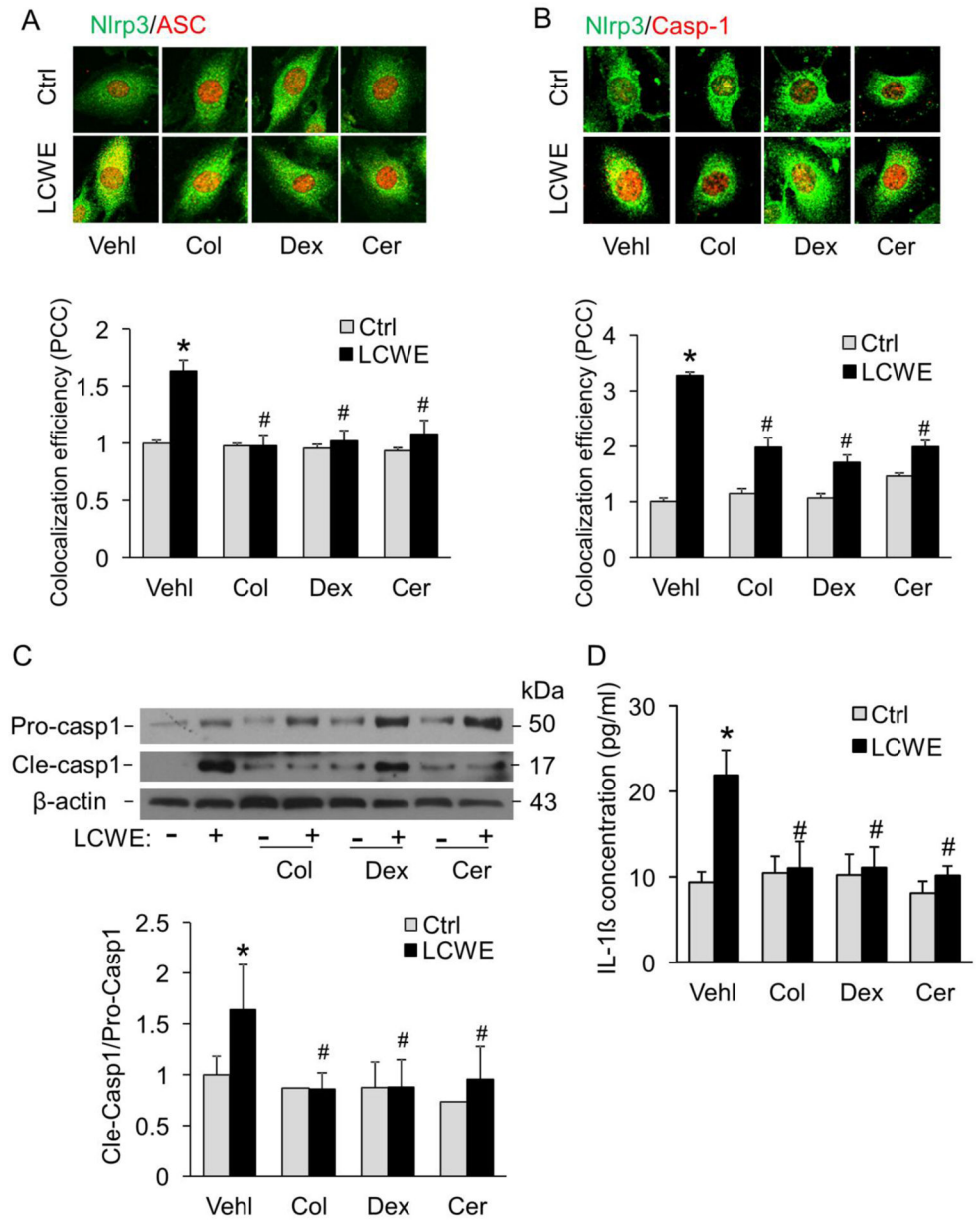

Fig. 6. LCWE-induced activation of Nlrp3 inflammasomes is associated with increased lysosome membrane permeability

MVECs were stimulated without (control: Ctrl) or with LCWE (10 μg/ml, 8 hour) in either the absence or presence of lysosomal function stabilization reagents (Vehl: vehicle only; Col: colchicine, 10 μM; Cer: C2-ceramide, 20 μM, Enzolife science; and Dex: dexamethasone, 100 μM, Sigma). (A) and (B) MVECs were stained with Alexa488-conjugated anti-Nlrp3 and Alexa555-conjugated anti-ASC or anti-caspase1 antibodies. Representative images show the colocalization (yellow) of Nlrp3 (green) with ASC (red) or Nlrp3 (green) with caspase-1 (red). Summarized data in panels A and B show the colocalization coefficiency of Nlrp3 with ASC or Nlrp3 with caspase-1 (n=5). (C) Western blot analysis of cleaved caspase-1 and pro-caspase-1 in MVECs (n = 6). (D) IL-1β

production in MVECs by ELISA (n = 6). * $P < 0.05$ vs. vehicle control; # $P < 0.05$ *vs.* vehicle+LCWE.

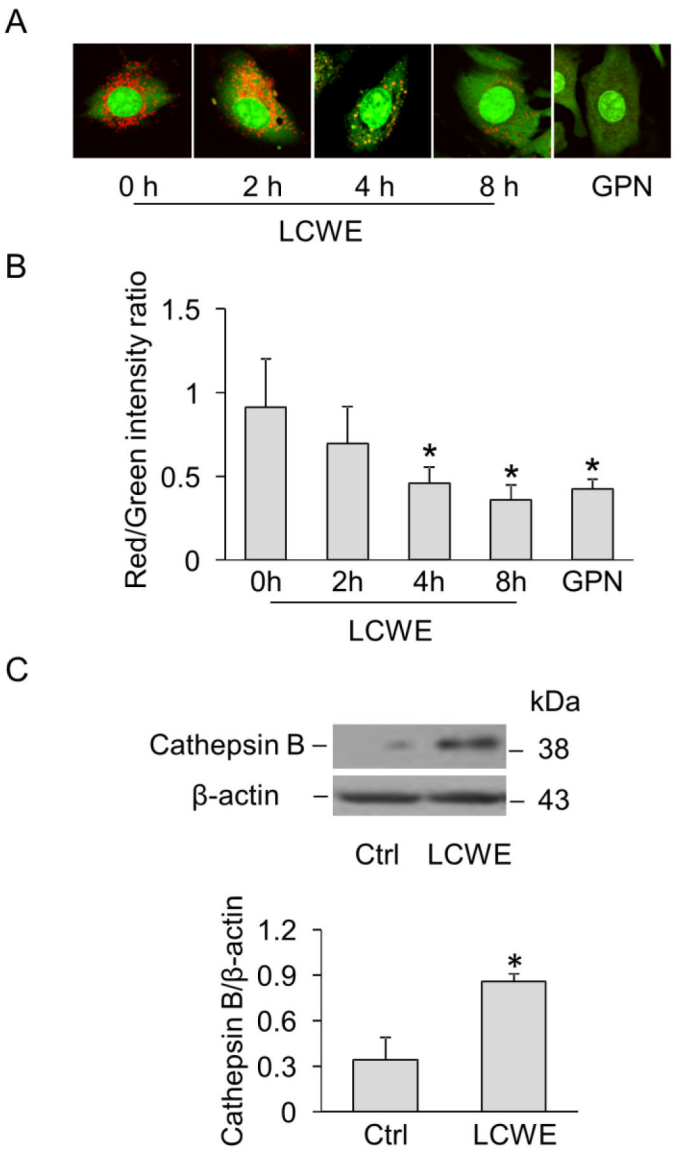

Fig. 7. LCWE increased lysosome membrane permeability and cathepsin B release in MVECs

(A) MVECs were incubated with either LCWE (10 μg/ml) for 0, 2, 4 and 8 hours or GPN (100 μM) for 4 h. Lysosome membrane permeability was detected by acridine orange staining and visualization by fluorescence microscopy. (B) Summarized data show the red-to-green fluorescence ratio of acridine orange staining in MVECs by flow cytometry analysis (n = 3). * $P < 0.05$ vs. LCWE 0 hour. (C) Western blot analysis of cathepsin B expression in cytosolic fractions of MVECs with or without LCWE (10 μg/ml, 8 h) (n = 5). * $P < 0.05$ vs. control.

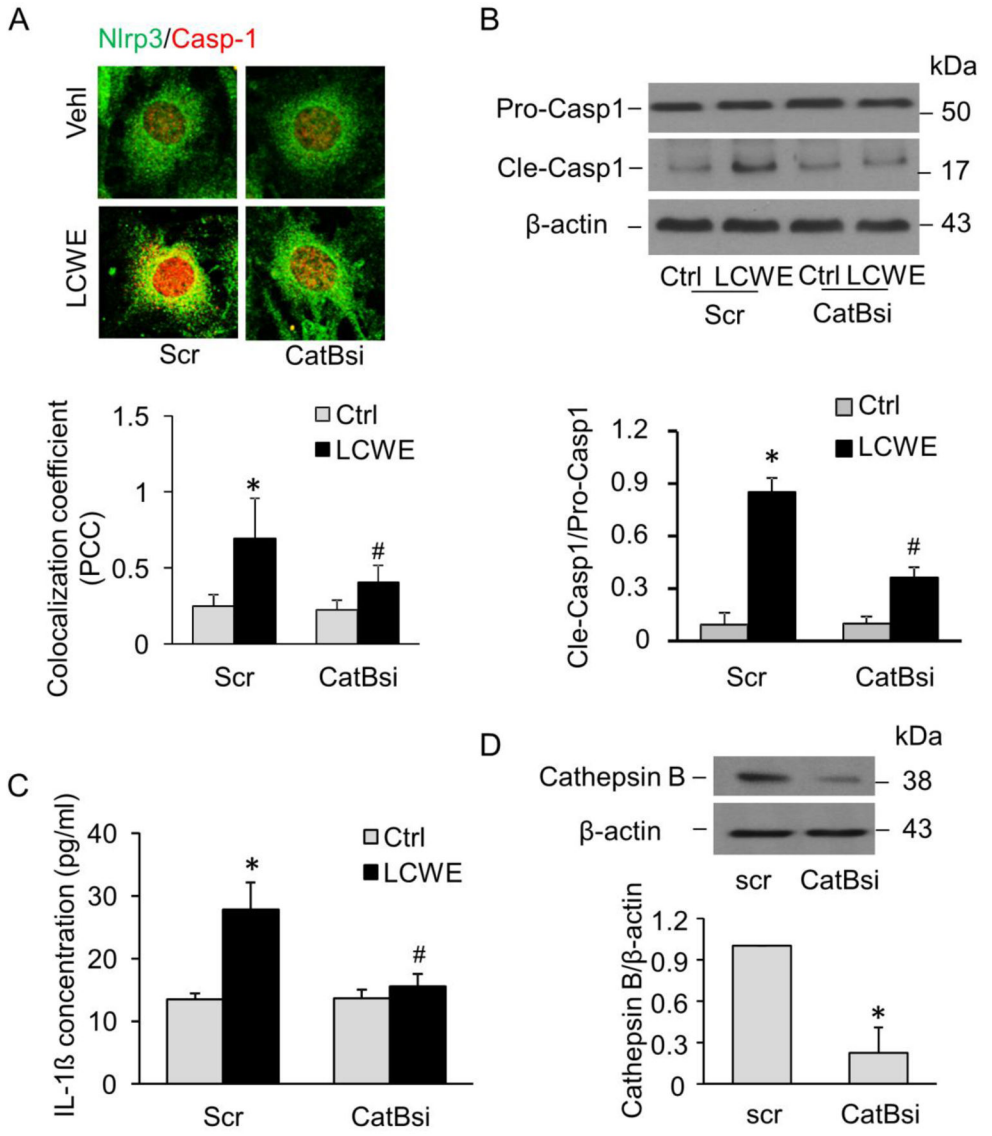

Fig. 8. Effects of cathepsin B gene silencing on LCWE-induced Nlrp3 inflammasome activation

MVECs were transfected with scramble (Scr) or cathepsin B siRNA (CatBsi) for 24 hours and then stimulated with or without LCWE (10 μg/ml, 8 h). (A) Confocal fluorescent images and summarized co-localization coefficient show the co-localization (yellow) between Nlrp3 (green) and caspase-1 (red) (n = 4). (B) Western blot analysis of cleaved caspase-1 and pro-caspase-1 (n = 4). (C) IL-1β production (n = 6). (D) Western blot analysis of cathepsin B expression in cell lysates of MVECs transfected with scramble or cathepsin B siRNA (n = 4). * $P < 0.05$ *vs.* scramble control; # $P < 0.05$ *vs.* scramble+LCWE.

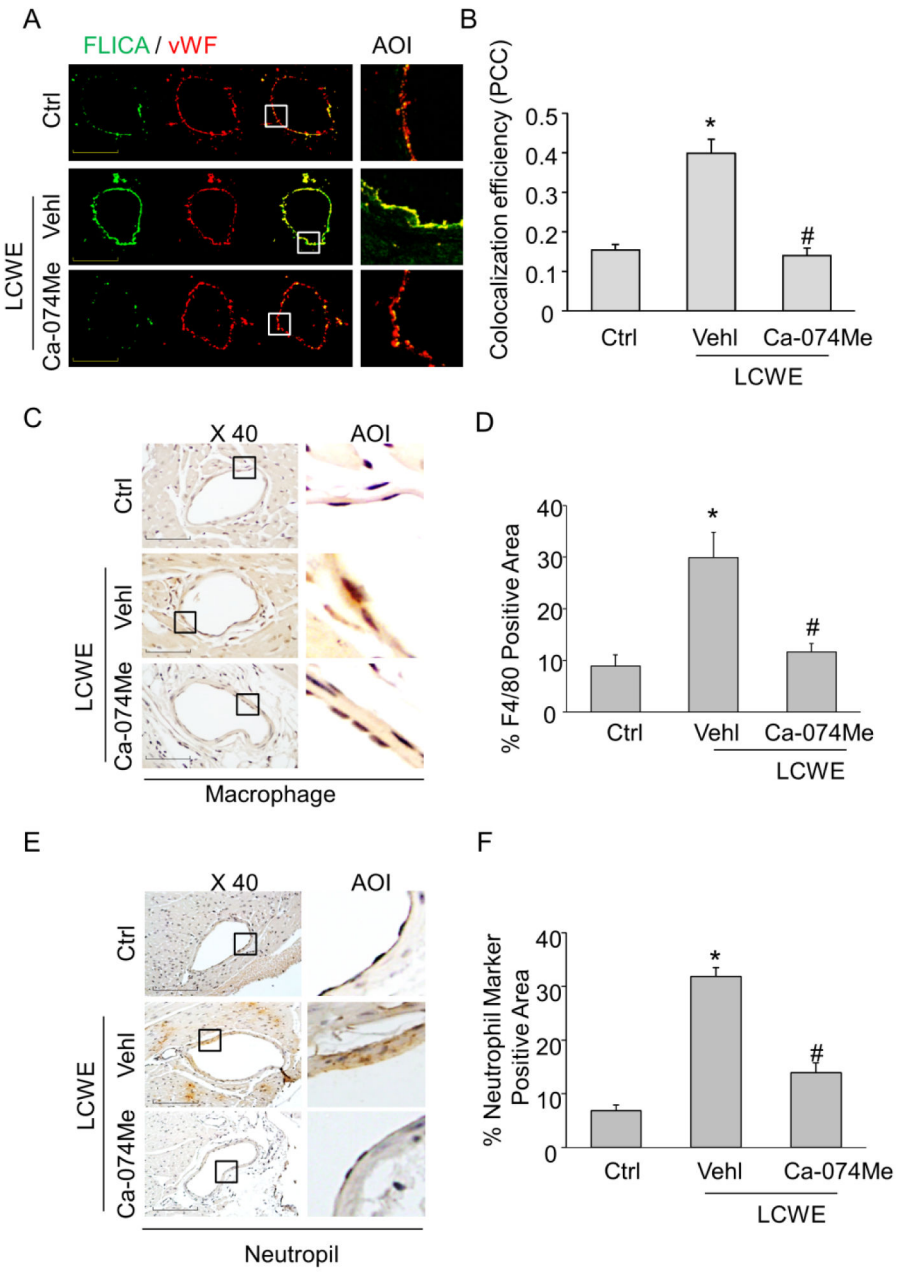

Fig. 9. Effects of cathepsin B inhibition on LCWE-induced inflammasome activity in coronary arterial endothelium of mice

Mice were intraperitoneally treated with saline control (Ctrl), LCWE (500 μg, 2 weeks) with or without cathepsin B inhibitor Ca-074Me (5mg/kg). (A) and (B) Frozen sections of mouse hearts were stained with FLICA, a green fluorescent probe specific for active caspase-1, and Alexa555-conjugated antibodies against an endothelial cell marker vWF in coronary arteries. The merged images displayed yellow dots or patches indicating the colocalization of FLICA (green) with vWF (red). Summarized data showing the colocalization coefficient of FLICA with vWF. (C) and (D) IHC staining showing the expression of macrophage marker F4/80 in the endothelium of coronary arteries. Summarized data showing area

percentage of the endothelium positive for F4/80 in coronary arteries. (E) and (F) IHC staining showing the expression of neutrophil marker in the endothelium of coronary arteries. Summarized data showing area percentage of the endothelium positive for neutrophil marker in coronary arteries. Enlarged images of area of interest (AOI) are indicated with an arrow. Scale bar: 50 μm. N = 5 mice per group. *P < 0.05 vs. control; # P<0.05 *vs.* LCWE only.